A model to extend spectral and multiwavelength UV irradiances time series: Model development and validation

Susana Díaz,[1] Don Nelson,[2] Guillermo Deferrari,[3] and Carolina Camilión[4]

Received 25 January 2002; revised 13 June 2002; accepted 8 August 2002; published 28 February 2003.

[1] Measurements of spectral and multichannel UV radiation became more common in the middle and late eighties after the discovery of the ''ozone hole,'' but time series for these measurements are still relatively short for the determination of trends to be applied in geophysical and biological studies. However, systematic measurements of total column ozone have been performed since the late 1950s at several stations, and global coverage has been available since the late 1970s. Also, long-term time series of broadband instruments (Pyranometers, UV and erythemally weighted) are available from many sites around the world. In this paper a multiregressive model that enables the inference of spectral or narrow band UV irradiances from total ozone column and broadband irradiance, in places where relatively short time series of UV spectral irradiances are available, is proposed. To test the model, measurements of irradiances performed at three of the stations in the NSF UV Radiation Monitoring Network, under all weather, solar zenith angle and surface conditions, were used. The model generated very good results over a wide variety of situations. Pyranometer data from the NOAA/CMDL surface radiation budget database for South Pole and Barrow Stations were used to estimate daily integrated narrow band irradiances. A time series of monthly means for the narrowband (303.030–307.692 nm) were then computed, dating back to the late 1970s. *INDEX TERMS:* 1630 Global Change: Impact phenomena; 1694 Global Change: Instruments and techniques; 3309 Meteorology and Atmospheric Dynamics: Climatology (1620); *KEYWORDS:* UV-B Irradiances, Ozone, Ozone depletion, UV irradiance modeling, Multiregressive model

Citation: Díaz, S., D. Nelson, G. Defarrari, and C. Camilión, A model to extend spectral and multiwavelength UV irradiances time series: Model development and validation, *J. Geophys. Res.*, *108*(D4), 4150, doi:10.1029/2002JD002134, 2003.

1. Introduction

[2] Measurements of spectral and multichannel UV radiation are important in determining the effects of atmospheric ozone depletion at the Earth's surface. Since these types of measurements became more common only after the discovery of the ''ozone hole,'' time series are still relatively short and many investigators have attempted to extend them in order to obtain databases suitable to study the effects of ozone depletion in the biosphere.

[3] Ground-level radiation is a function of several factors: Sun-Earth distance, atmospheric gases and aerosols, solar zenith angle, clouds, altitude and surface albedo. Geometric factors (solar zenith angle and the Earth-Sun distance) are very important in determining irradiances at the Earth's surface, and variability of irradiances as a function of these parameters is well established. The irradiance variations with time of the day, latitude and season result from a change in the solar zenith angle. As consequence of the variation in the Earth-Sun distance, extraterrestrial radiation is 7% higher when summer solstice occurs in the Southern Hemisphere, than during the Northern hemisphere summer solstice [*Frölich*, 1987].

[4] Stratospheric ozone is the most important atmospheric gas affecting ground-level UV irradiances and exhibit both temporal and geographical variations. Higher ozone values are typically observed at higher latitudes and lower values in the tropical regions. Main temporal variations of this parameter include a seasonal cycle, which is more pronounced at high latitudes than at low latitudes, and day-to-day variations. There are also temporal changes related to the quasibiennial oscillation (QBO) [*Huang*, 1996; *Randell and Wu*, 1996; *Zerefos et al.*, 1998] and the 11-year sunspot cycle and the 27-days Sun rotation [*Chandra and McPeters*, 1994; *Lean et al.*, 1997; *Zhou et al.*, 1997; *Callis et al.*, 2000; *Zhou et al.*, 2000]. Short-term predictions of total column ozone with some accuracy are possible over specific sites, and estimation of long-term depletion on regional scales is also possible. The dependence of ground-level UV radiation on other atmospheric parameters such as aerosols is under study [*Erlick and Frederick*, 1998; *Kylling et al.*, 1998a; *Ilyas et al.*, 2001], and satellites have enabled global

[1]Centro Austral de Investigaciones Científicas/CONICET, Ushuaia, Tierra del Fuego, Argentina.
[2]National Oceanic and Atmospheric Administration/CMDL, Boulder, Colorado, USA.
[3]Centro Austral de Investigaciones Científicas/NSF, Ushuaia, Tierra del Fuego, Argentina.
[4]Centro Austral de Investigaciones Científicas/IAI, Ushuaia, Tierra del Fuego, Argentina.

0148-0227/03/2002JD002134$09.00

scale measurements of this parameter only in recent decades [*Herman et al*, 1997; *Krotkov et al.*, 1998].

[5] The presence of clouds may be responsible for large changes in the irradiance at the Earth's surface and their effect is described by Mie scattering theory. Usually, clouds attenuate the UV, although under broken cloud conditions, an increase of up to 27% above clear sky values may be observed [*Frederick and Steele*, 1995; *Estupinan et al.*, 1996]. This effect seems to be related to the vertical extent of the cloud field [*Wardle et al.*, 1997]. Cloud optical properties impact on the irradiance is complex; nevertheless, simple relationships have been developed to calculate the attenuation of irradiance in presence of clouds [*Mo and Green*, 1974; *Cutchis*, 1980; *Josefsson*, 1986; *Illyas*, 1987; *Frederick and Steele*, 1995; *Chubarova et al.*, 1997; *den Outer et al.*, 2000]. Sometimes the presence of clouds may mask ozone depletion. For example, strong ozone depletion observed during overpass of the ozone hole in presence of cloudy skies and high solar zenith angles, produced lower irradiances than weaker ozone depletions on clear days, near the summer solstice [*Diaz et al.*, 1994].

[6] The above discussion suggests that inference of past UV spectral irradiances is problematic, in some cases because of the complexity of the relation between the UV and the parameter, and in others because of the lack of information on the variability of the parameter itself. Algorithms have been developed to retrieve UV radiation at the Earth's surface from satellite data. The irradiance values are calculated using derived values of ozone and aerosol amounts, cloud and ground reflectivity, and extraterrestrial solar flux [*Cebula et al.*, 1994; *Eck et al.*, 1995; *Cebula et al.*, 1996; *Li et al.*, 2000].

[7] Alternatively, some methodologies have been proposed to infer spectral irradiances from broadband measurements. They allow extension of spectral time series through the use of longer broadband irradiance time series from networks of well-calibrated instruments. *Ito et al.* [1994] developed an empirical model to derive daily integrated UV-B irradiances from daily integrated global solar radiation via an equation, which includes total ozone column and solar zenith angle. *Bodecker and McKenzie* [1996] proposed a semiempirical model based on meteorological variables and total column ozone. The algorithm includes measured broadband irradiance and clear sky erythemal and broadband irradiance calculated using (1) a statistical derivation from measured data and (2) the output of a surface spectral irradiance model. *Fioletov et al.* [2000] developed a statistical model to derive spectral UV-B and spectrally weighted irradiances from global solar radiation, in two steps: (1) estimation of UV-A (324 nm) from global radiation and (2) estimation of spectral UV-B or spectrally weighted irradiance from irradiance at 324 nm. The model also considered other parameters such as total ozone, a cloud factor, clear sky irradiance at 324 nm and the cosine of the solar zenith angle [*Fioletov et al.*, 1997; *McArthur et al.*, 1999].

[8] In this paper a multiregressive model is proposed, which can be used to estimate spectral, narrowband or biologically weighted irradiances in places where long time series of broadband measurements (UV-B, UV-A, UV-B biologically weighted, pyranometer) are available. The model discussed in this paper is very simple and, in spite of that, it showed very good results. The model only needs irradiance measured by broadband instruments and ozone total column; it also considers SZA, which can be calculated by a simple algorithm. Since ozone can be provided by ground-based instrumentation, an advantage regarding to the algorithms that involve satellite data is that irradiance values prior to satellite ozone measurements (1978) can be inferred. Also, no additional models are necessary, or considerable computational resources. Since the same methodology can be applied to different types of broadband instruments, it would also be possible to convert time series of several independent well-calibrated broadband instruments of different types into a network, creating a database of spectral or narrow-band irradiances, just adding a spectral or multichannel travelling instrument, which would be used to determine the regression coefficients.

2. Data and Methodology

[9] The model was derived from a regression analysis performed to determine the contribution of geometric factors, clouds and ozone, jointly and separately, in the variability of biologically effective irradiances at Ushuaia [*Diaz et al.*, 2000]. Assuming that the variation in biologically effective irradiances may be considered as the product of the variation associated with clouds and geometric factors and an attenuation factor related to ozone changes, a simple and a multivariate regression analysis of biologically weighted daily integrated irradiances versus total column ozone and daily integrated irradiances in the band 337–342 nm based on Lambert-Beer Law was performed by *Diaz et al.* [2000]. In that study, the band 337.5–342.5 nm was considered an indicator of the variations of clouds and geometric factors since (1) irradiances in the UV-A, wavelengths above 320 nm, may be considered independent of ozone changes; (2) although a wavelength dependence in cloud transmittance has been reported [*Seckmeyer et al.*, 1996; *Frederick and Erlick*, 1997; *Kylling et al.*, 1998b], as a first approach, it may be considered that clouds have a similar behavior in the UV-B and UV-A; and (3) geometric factors affect both UV bands, although with different magnitude [*Diaz et al.*, 2000]. From the previous paragraph, orthogonality of the selected variables is clear, since irradiances in the band 337.5–342.5 nm are independent of ozone and vice versa. This is also reflected by the low R^2 between the two variables ($0.004 < R^2 < 0.06$, depending on the month).

[10] Taking into account that an exponential relationship is observed between biologically effective irradiances and UV-A irradiances, which is a consequence of the dependence of the first one on total column ozone, while the irradiances in the UV-A are independent of it, the proposed multivariate equation was

$$ln\ E_s = a_1\ ln\ E_b + a_2 O_3 + b \quad (1)$$

where E_s is the biologically weighted daily integrated irradiance; E_b is the 337.5–342.5 nm daily integrated irradiance; O_3 is the total column ozone (daily value); and a_1, a_2, and b are the regression coefficients, determined using least squares methods.

[11] Based on the results of the analysis, a multiregressive model was, then, proposed to estimate biologically weighted

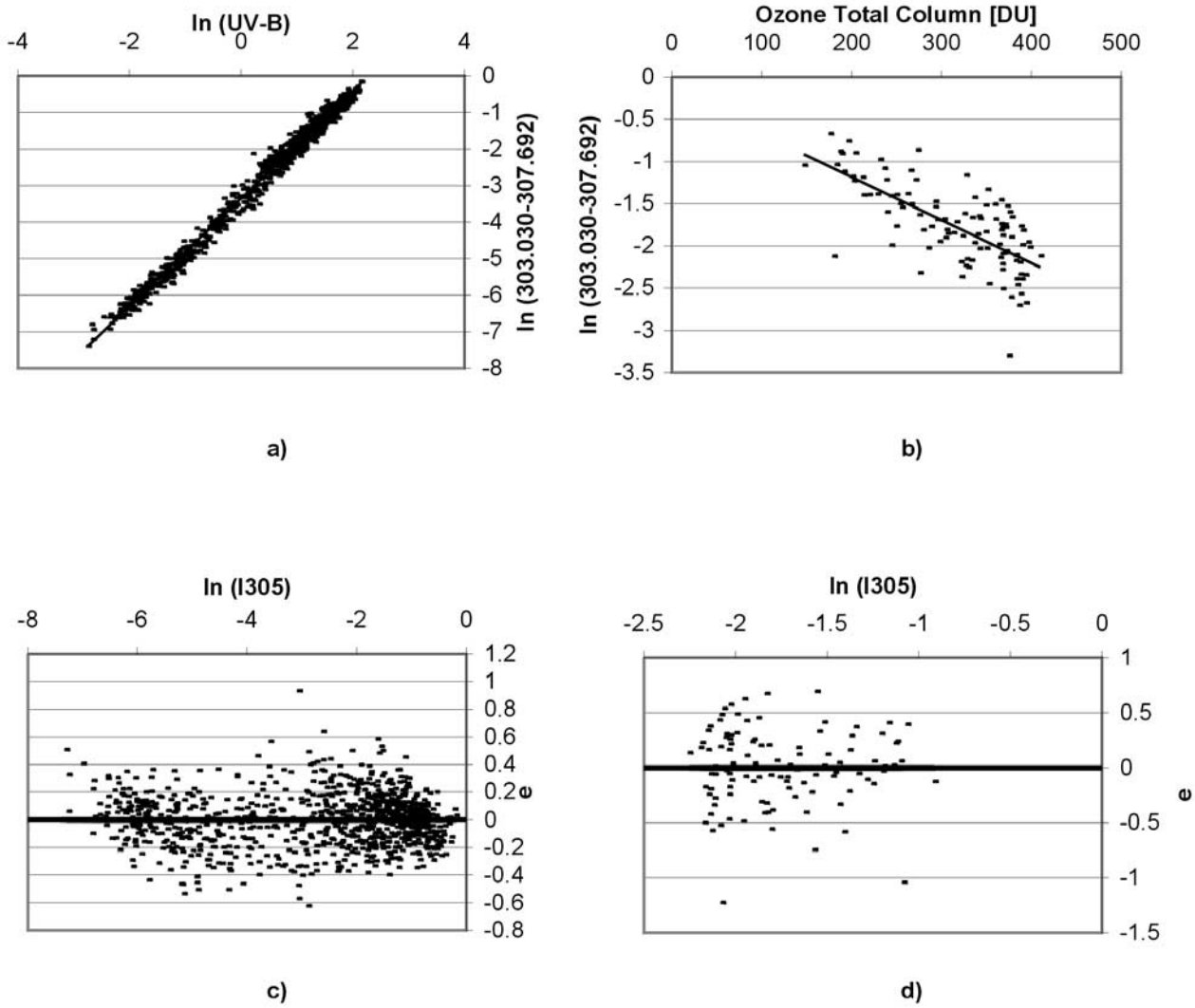

Figure 1. Linear relationship of the logarithm of daily integrated irradiances in the band 303.030–307.692 nm versus (a) the logarithm of daily integrated UV-B and (b) ozone total column for Ushuaia. (c, d) Homoscedasticity of the residuals. Since the correlation of irradiance 303.030–307.692 nm with ozone is very low, except when large ozone changes occur; only data for October is shown in Figures 1b and 1d.

irradiances as function of a narrow UV-A band and total column ozone. Instruments measuring solar irradiance usually do not integrate in a narrow band as 337.5–342.5 nm, except for spectroradiometers; thus, it was considered that the proposed model needed to be modified and tested under more general and realistic conditions to be practical.

[12] In the present paper, the multiregressive model has been adapted to infer biologically weighted, spectral or narrow-band UV-B irradiance, using as a proxy for clouds broadband instruments measurements (for example, UV-B or erythemally weighted irradiance). In Figure 1, validity of the relationships proposed in equation (1) for this new approach is shown. Figures 1a and 1b show scatterplots of the logarithm of daily integrated irradiance in the band 303.030–307.692 nm versus the logarithm of daily integrated UV-B (Figure 1a) and ozone total column (Figure 1b) for Ushuaia, where linearity of the proposed relationships is observed. Homoscedasticity of the residuals is also clear, which is confirmed in Figures 1c and 1d, where an even distribution of the residuals is observed as a function of the logarithm of the estimated irradiance in the band 303.030–307.692 nm. Since, as concluded by *Diaz et al.* [2000], the correlation of biologically weighted irradiance (in this case 303.030–307.692 nm) with ozone is very low, except when large ozone changes occur, in Figures 1b and 1d only data for October are shown, since otherwise it would not be possible to observe any relationship.

[13] When testing the model using visible or global irradiances as a proxy for clouds, it was empirically determined that, in those cases, better results were obtained when adding the solar zenith angle as one of the variables. Then, equation (1) was modified as follows:

$$ln\ E_S = a_1\ ln\ E_b + a_2 O_3 + a_3\ \varphi + b \qquad (2)$$

where E_s is spectral, narrowband or biologically weighted daily integrated irradiance; E_b is broadband daily integrated

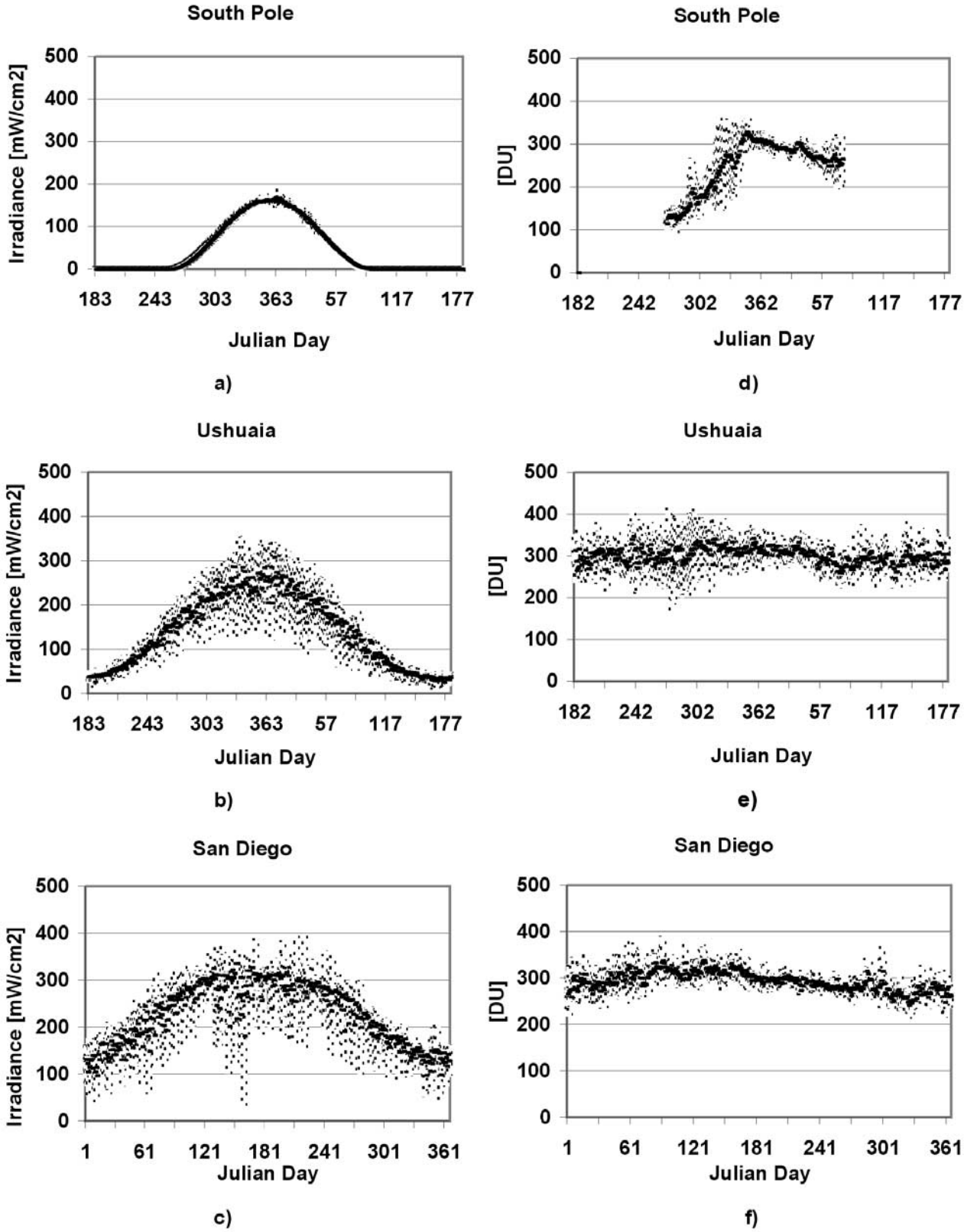

Figure 2. (a, b, c), Historical mean (1991–1997) and standard deviation of the maximum daily values for the band 337.5–342.5 nm, as a proxy for cloud cover. (d, e, f) Historical mean and standard deviation of daily total column ozone.

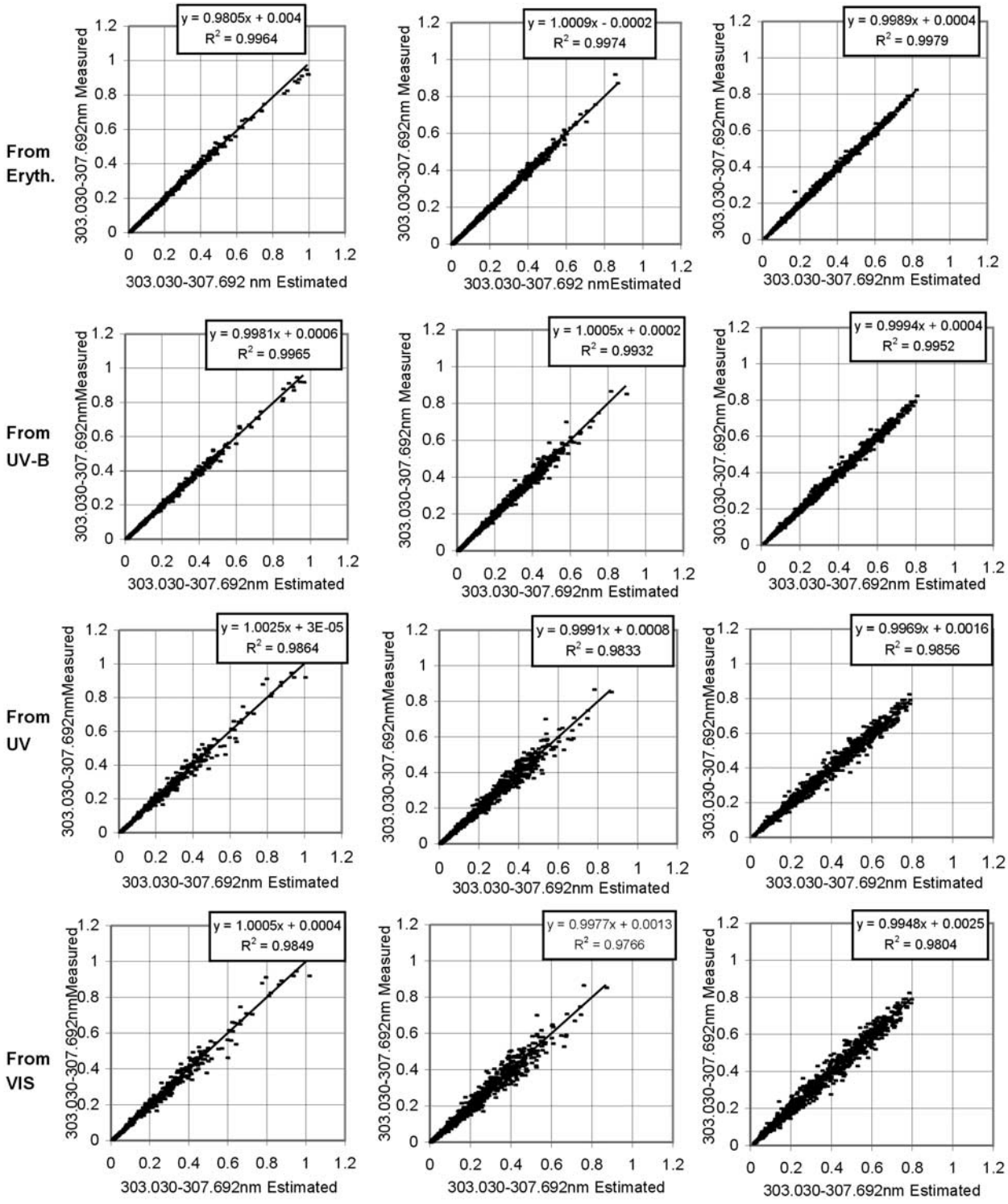

Figure 3. Daily integrated irradiances, measured and estimated from different bands.

irradiance; O_3 is total column ozone (daily value); φ = solar zenith angle averaged daily value, and a_1, a_2, a_3 and b are the regression coefficients, determined using least squares methods.

[14] When using broadband measurements, instead of the band 337.5–342.5 nm, orthogonality of the variables needs to be tested, since the band proposed as a proxy for clouds, in this case, includes information on ozone variability and the relevance of that information will vary with the integrated band (for example, the erythemally weighted irradiance will provide more information on ozone changes than the irradiance measured with a pyranometer). The R^2 for pyranometer and erythemally weighted irradiances with ozone total column were calculated to test orthogonality

Table 1. Relative Error, RMS, in Percent, for the Estimated Daily Integrated Irradiances and for Monthly Mean Daily Integrated Irradiances, Narrowband 303.030–307.692 nm, Calculated From SUV-100 Broadband Simulated[a]

	Erythema	UV-B	UV	Visible
		Daily		
South Pole	$4.17_{(0.9964)}$	$4.28_{(0.9965)}$	$8.12_{(0.9864)}$	$8.66_{(0.9849)}$
Ushuaia	$5.79_{(0.9974)}$	$6.07_{(0.9932)}$	$10.96_{(0.9833)}$	$14.55_{(0.9766)}$
San Diego	$3.63_{(0.9979)}$	$4.66_{(0.9952)}$	$8.37_{(0.9856)}$	$10.11_{(0.9804)}$
		Monthly Mean		
South Pole	$1.54_{(0.9983)}$	$1.95_{(0.9978)}$	$2.50_{(0.9985)}$	$2.85_{(0.9978)}$
Ushuaia	$1.35_{(0.9998)}$	$1.58_{(0.9997)}$	$3.20_{(0.9983)}$	$3.51_{(0.9980)}$
San Diego	$1.43_{(0.9996)}$	$1.84_{(0.9991)}$	$3.39_{(0.9970)}$	$4.42_{(0.9948)}$

[a]R^2 is provided in brackets.

of the variables. In the first case, the R^2 were low and were nonstatistically significant (bellow 0.02), while for the erythemally weighted irradiance the R^2 varied between 0.0004 and 0.27. In both cases a few larger values were observed, but, since 337.5–342.5 nm (independent of ozone) showed about the same value of R^2 when correlated with ozone, then, the observed relationship results, indeed, from a coincidence between ozone and cloud variations. From the previous results it is concluded that the orthogonality of the variables can still be considered valid.

[15] In the work of *Diaz et al.* [2000] the band 337.5–342.5 nm was used as proxy for clouds, assuming that, as first approach, clouds transmittance can be consider the same in the UV-B and UV-A. In the present paper a more general situation is considered, where even pyranometer measurements are proposed as clouds proxy. To test the validity of this approach, the R^2 for 337.5–342.5 nm and visible irradiances were calculated, and values were above 0.97 for all sites. Also, where available, the R^2 for 337.5–342.5 nm and pyranometer measurement were calculated; in this case the values were above 0.96. Then, it is concluded that pyranometer measurements can be considered a proxy for clouds as good as 337.5–342.5 nm.

[16] The model was tested for different locations, presenting a variety of situations regarding to ozone and cloud cover and, also, variability of the results with wavelength was analyzed.

[17] The multiregressive model was solved to compute daily integrated irradiances for the period January 1993 through December 1998 for Ushuaia (54°49′S, 68°19′W), South Pole (90°S, 0°) and San Diego (32°45′N, 117°11′W), using yearly data under all weather conditions, which included different cloud covers, solar zenith angles and albedo situations. Then, using the regression coefficients obtained from this period, the model was tested for the time series January 1992 through June 2000 for South Pole and Ushuaia, and November 1992 through August 2000 for San Diego.

[18] The selected sites show important differences in the patterns of ozone and cloud variability (Figure 2). Ushuaia experiences large daily ozone variations during the spring because of the presence of the "Ozone Hole" and is under rather cloudy skies. South Pole experiences the "Ozone Hole" at the beginning of the spring and remains in that condition for most of that season, under fairly clear skies. Finally, San Diego is a typical midlatitude site.

[19] To avoid the contribution of errors generated by instrument differences, such as collector response and calibration, the model was first tested using both, spectral and broadband irradiances, obtained from the NSF UV Radiation Monitoring Network. Details on the Network and the spectroradiometer SUV–100 are described in several publications [*Booth et al.*, 1994, 1998].

[20] As a second step, the Eppley UV Radiometer (TUVR) and Eppley Pyranometer (PSP), which are mounted as auxiliary sensors side by side with the SUV-100 spectroradiometers at South Pole and Ushuaia, were used as source for the broadband irradiances. Finally, data from the CMDL surface radiation budget monitoring program at South Pole and Barrow were used to test the model and estimate narrowband irradiances back to the latter part of 1978.

[21] The irradiances from the NSF UV Radiation Monitoring Network were provided by Biospherical Instruments Inc. (C. R. Booth, NSF UV Radiation Monitoring Network, volumes 1-6, 1992–2000 (available at http://www.biospherical.com/nsf/index.asp)). The broadband simulated irradiances from the SUV–100 were obtained from Database 3, where they were calculated integrating the spectral measurements in 1-nm steps. From this database we selected erythemally weighted irradiances, UV-B, UV and a band in the visible, as simulations of broadband instruments. In the case of the erythemally weighted irradiances the weighting function simulated the response of a biometer, then, the effective irradiance, was calculated as

$$I = \int_{\lambda_1}^{\lambda_2} I_\lambda(\lambda)\, W_\lambda\, d\lambda \qquad (2')$$

where I is the biologically effective irradiance ($\mu W/cm^2$), $I_\lambda(\lambda)$ is the irradiance at wavelength λ($\mu W/cm^2$/nm), (λ) is the weighting function (action spectrum) dimensionless, λ_1 is 290 nm and λ_2 is 400 nm. In Database 3 the integration is replaced by summing in 1-nm steps.

[22] There are two definitions for the UV-B band: (1) 290–315 nm and (2) 290–320 nm; although many photobiologists prefer the first one, in this study we have chosen the second, since we wanted to check the model under a broad variety of situations, and we considered that the band 290–315 nm would give a very similar result to erythemally weighted irradiances. Also, since the largest wavelength scanned by the SUV-100 is 620 nm, only the band 400–600

Table 2. Relative Error, RMS, in Percent, for the Estimated Daily Integrated Irradiances, at Different Narrowbands, Calculated From SUV-100 Broadband Simulated Erythemally Weighted and Visible Irradiances[a]

	298.507–303.030 nm	303.030–307.692 nm	307.692–312.500 nm	312.500–317.500 nm
From erythema	$7.20_{(0.9941)}$	$3.63_{(0.9979)}$	$2.01_{(0.9988)}$	$2.34_{(0.9974)}$
From visible	$14.04_{(0.9749)}$	$10.11_{(0.9804)}$	$7.74_{(0.9836)}$	$6.22_{(0.9874)}$

[a]R^2 is provided in brackets.

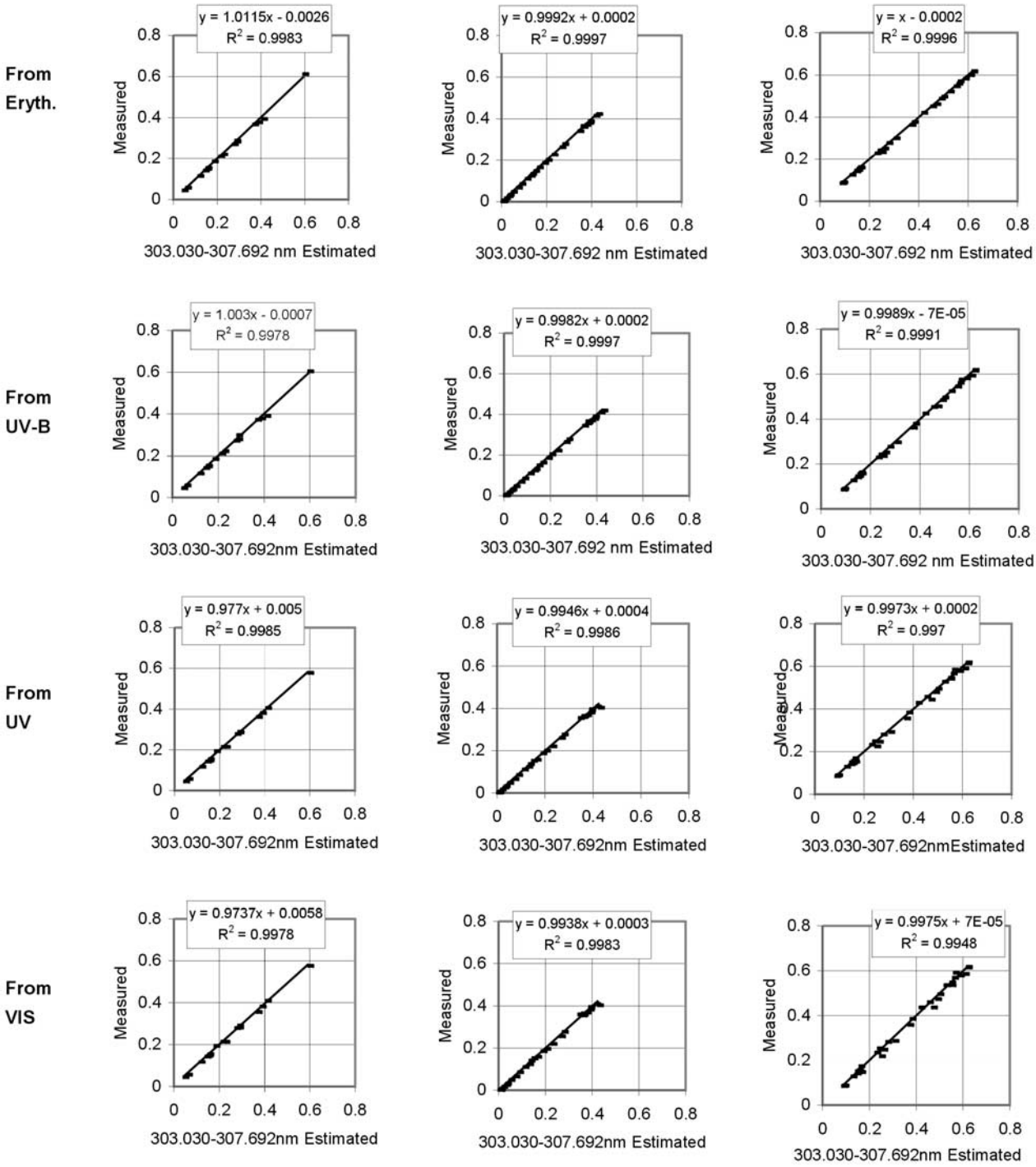

Figure 4. Daily integrated irradiances monthly mean, measured and estimated from different bands.

nm was considered in the visible. Finally, the UV band is the summation of UV-B and UV-A (290-400 nm).

[23] Total column ozone was provided by NASA Goddard Space Flight Center [*McPeters and Beach*, 1996, 2000; *McPeters et al.*, 1996, 1998; R. McPeters and E. Beach, TOMS Nimbus-7 and Meteor-3, version 7, 1996 (available at http://toms.gsfc.nasa.gov); R. McPeters and E. Beach, TOMS Earth-Probe, 2000 (available at http://toms.gsfc.nasa.gov); J. Herman, ADEOS TOMS, version 7, User's Guide, 1998 (available at http://toms.gsfc.nasa.gov)]. Data are available from three different satellites dating back to 1978, with a gap between January 1995 and September 1996, winter gaps in South Pole and some additional minor gaps.

[24] Broadband pyranometer data collected by NOAA/CMDL at South Pole from January 1976 to December 1998 (with a few minor gaps) were also available.

[25] When solving the model, it was observed that better results were obtained when data were grouped by month. Using monthly data, the error in the regression equation coefficients diminished, particularly in winter months, since

Table 3. Relative Error, RMS, in Percentage, for Daily Integrated and Monthly Mean of Daily Integrated Irradiances, Narrowband 303.030–307.692 nm, Calculated From SUV-100 Broadband Simulated[a]

	Erythema	UV-B	UV	Visible
		Daily		
South Pole	$5.71_{(0.9964)}$	$5.49_{(0.9968)}$	$10.36_{(0.9852)}$	$10.29_{(0.9835)}$
Ushuaia	$6.42_{(0.9971)}$	$6.45_{(0.9935)}$	$11.96_{(0.9836)}$	$15.69_{(0.9760)}$
San Diego	$3.56_{(0.9980)}$	$4.70_{(0.9952)}$	$8.99_{(0.9833)}$	$11.00_{(0.9758)}$
		Monthly Mean		
South Pole	$2.75_{(0.9985)}$	$2.90_{(0.9984)}$	$5.06_{(0.9929)}$	$5.50_{(0.9915)}$
Ushuaia	$2.55_{(0.9991)}$	$2.49_{(0.9988)}$	$3.58_{(0.9976)}$	$4.29_{(0.9978)}$
San Diego	$1.47_{(0.9995)}$	$1.93_{(0.9989)}$	$4.17_{(0.9948)}$	$5.49_{(0.9910)}$

[a]For the period January 1992 through June 2000 for South Pole and Ushuaia, and November 1992 through August 2000 for San Diego, using the model developed for 1993–1998. R^2 is provided in brackets.

they do not contribute significantly when included with other seasons at the moment of applying least squares.

[26] After daily integrated values were modelled, monthly mean values for measured and estimated daily values were calculated and compared. Months with 15 days, or more, of available data were used to evaluate the RMS relative error and R^2.

3. Results

3.1. Spectral From SUV-100

[27] The narrowband (303.030–307.692 nm) was estimated solving the regression equation for the period 1993–1998 from the following broadband data: UV-B (290–320 nm), UV (290–400 nm), UV erythemally weighted, and the portion of the visible measured by the SUV-100 (400–600 nm). The scatterplots for measured and inferred irradiances are illustrated in Figure 3. The equations of the regression lines relating measured and estimated values exhibit negligible effects of systematic over or under estimation of the model (b near zero and slope near 1).

[28] The RMS relative errors in percentage and R^2 are listed in Table 1. The results are consistent with the cloud and ozone patterns mentioned above. At Ushuaia, the site with higher error and lower R^2, higher complexity in the behavior of both parameters is present. This location also possesses the highest variability in the albedo and, since this parameter is not considered in the model, it can contribute to increase the error. In all cases the best results were obtained for values inferred from UV–B and erythemally weighted irradiances, and the higher errors were associated with values derived using the visible data, as could be expected.

[29] A statistical analysis of the significance of the coefficients of the regression equation was performed using the $c_{ritical}$ test, which determines if the parameter selected is an important variable when estimating the spectral irradiance. The results suggest that all of the coefficients of the regression equation are significant ($\alpha = 0.01$). When the analysis was performed grouping the days by month, the coefficient for solar zenith angle (SZA) shows less significance in those months where that parameter presents a small variation during the period (for example, December or June in Ushuaia). Also, at South Pole, due to the relatively lower cloud amount [*Warren et al.*, 1986], and hence fewer cloudy sky irradiance cases, the coefficient for the broadband irradiance (cloud indicator) is comparatively less significant. In contrast, the same coefficient shows the highest significance in Ushuaia, where the presence of clouds is very important. The coefficient for SZA is more significant when broadband visible irradiances are used than for erythemally weighted irradiances, as discussed above. This is because the variation imposed by this parameter in the erythemally weighted data is very similar to the variation in the 303.030–307.692 nm data. Finally, the $F_{critical}$ test shows that the results are statistically significant for $\alpha = 0.01$.

[30] In order to study the variability of these results with the wavelength of the estimated irradiance, a variety of daily integrated narrowband irradiances were calculated from erythemally weighted and visible broadband irradiances at San Diego. The results are tabulated in Table 2 where it is observed that the minimum error for the irradiance modelled from the erythemally weighted irradiance is observed near the peak of the weighted irradiance, and for values modelled from the visible band, the error diminishes as the wavelength increases, as could be predicted in both cases.

[31] The monthly mean values for the measured and estimated daily integrated irradiances were calculated. The scatterplots for the monthly mean of the measured and inferred daily integrated irradiances for the narrowband (303.030–307.692 nm) are shown in Figure 4. The RMS relative errors in percent, for months with 15 or more days, and the R^2 are shown in Table 1. The results show that the model is suitable for use in estimating irradiances to determine trends.

[32] Regression coefficients computed for the 1993–1998 period were used to test the model for the period January 1992 through June 2000 for South Pole and Ushuaia, and November 1992 through August 2000 for San Diego, except for the period where satellite ozone is not available (mainly all 1995 and part of 1996), and some minor gaps. The results are summarized in Table 3, where some increase is observed in the errors, particularly in the high–latitude sites, but the values still make them suitable for the use in trend analysis.

3.2. Spectral From Eppley SUV-100

[33] The TUVR instrument is an Eppley UV Radiometer provided with a Teflon collector that follows Lambert cosine response, with an encapsulated interference filter that limits the bandwidth to the range 295 to 385 nm. The PSP instrument is an Eppley Pyranometer provided with

Table 4. Relative Error, RMS, in Percentage, for Estimated Daily Integrated Irradiances and Monthly Mean of These Irradiances, Narrowband 303.030–307.692 nm, Calculated From Eppley UVP and PSP(1993–1998) and Extended to 1992–2000[a]

	Daily		Monthly	
	UVP	PSP	UVP	PSP
		1993–1998		
South Pole	$8.44_{(0.9832)}$	$8.55_{(0.9832)}$	$3.13_{(0.9977)}$	$2.90_{(0.9977)}$
Ushuaia	$11.85_{(0.9860)}$	$15.50_{(0.9785)}$	$4.66_{(0.9985)}$	$5.57_{(0.9943)}$
		1992–2000		
South Pole	$9.54_{(0.9851)}$	$9.82_{(0.9851)}$	$4.86_{(0.9964)}$	$5.09_{(0.9965)}$
Ushuaia	$13.37_{(0.9846)}$	$16.85_{(0.9779)}$	$5.10_{(0.9976)}$	$5.60_{(0.9936)}$

[a]R^2 is provided in brackets.

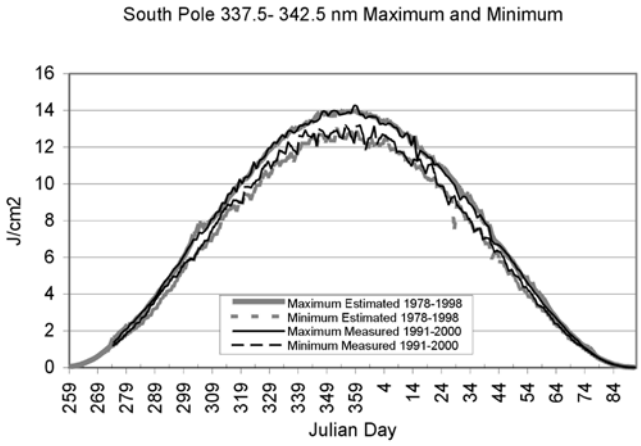

Figure 5. Maximum and minimum historical values for each Julian Day for irradiance 337.5–342.5 nm, used as a proxy for cloud attenuation, measured by spectroradiometer SUV-100/NSF (1991–2000), and estimated from CMDL/NOAA pyranometer data (1978–1998), at South Pole.

two hemispheres of Schott optical glass (WG295), which have a flat transmittance between 285 to 2800 nm. These instruments are calibrated on a yearly basis by Biospherical Instruments Inc., while the site visit of the SUV-100 is performed. Only two of the three stations considered in this study, Ushuaia and South Pole, have these instruments available as part of the system.

[34] The model was used to infer the band (303.030–307.692 nm) from the broadband irradiance measurements obtained from each of these instruments. The results for the period 1993–1998 and the extended period (1992–2000) are summarized in Table 4. The errors are, in general, slightly higher but similar to those obtained for the SUV-100 for the UV and visible bands. Both daily integrated and monthly means show higher errors for Ushuaia than for South Pole, and the causes for this have been discussed in section 3.1. It was observed that in some cases, when the regression coefficients had slightly lower values, it was related to the fact that the pyranometer was covered with snow, while the SUV was free of snow due to the heated collector.

3.3. Spectral Broadband Irradiances

[35] As an example of the possibilities of the model, the algorithm was applied to extend time series of narrowband irradiances at South Pole and Barrow. Pyranometers deployed by the NOAA/CMDL at their South Pole and Barrow (Alaska) baseline stations were characterized and calibrated at the NOAA/CMDL Solar Radiation Facility in Boulder Colorado. The pyranometers used by NOAA/CMDL are of the double dome type, with a single black detector, and each pyranometer was characterized for angular and temperature response. The CMDL sensors were selected for optimal operation at high latitudes. All calibrations are traceable to absolute cavity radiometers, which are in turn traceable to the World Radiometric Reference (WRR) in Davos Switzerland [*Nelson*, 2000].

[36] Using spectral data from the NSF UV Radiation Monitoring Network and broadband data from the NOAA/CMDL solar radiation database, the regression model was solved for South Pole and Barrow for the period 1993–1998. At South Pole, the differences between measured and estimated spectral daily integrated irradiances in the (303.030–307.692 nm) band resulted in an R^2 of 0.9833 and a RMS error of 8.58%, while for the monthly means the R^2 was 0.9964 with a RMS error of 3.28%; for Barrow the values were R^2 = 0.9839 and a RMS error = 15.25% for daily integrated irradiance, and R^2 = 0.9980 and RMS error = 4.07% for monthly means. The higher error observed in daily integrated values for Barrow are related to a larger variability in cloud conditions at this site.

[37] To test if the observed agreement between measured and estimated values could be extrapolated to infer values back to 1978 accurately, the model was solved for the band 337.5–342.5 nm for South Pole. Since this site shows relatively low cloud cover, no large interannual variation for wavelengths independent of ozone should be observed, unless a trend in cloud cover is occurring. In Figure 5, historical maximum and minimum values for each Julian

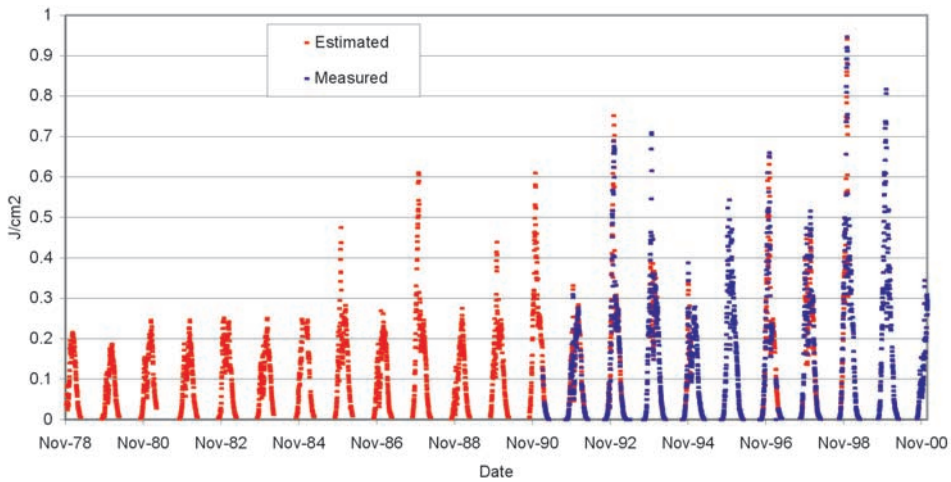

Figure 6. Daily integrated irradiance 303.030–307.692 nm estimated from CMDL/NOAA pyranometer and measured by spectroradiometer SUV-100/NSF, when available.

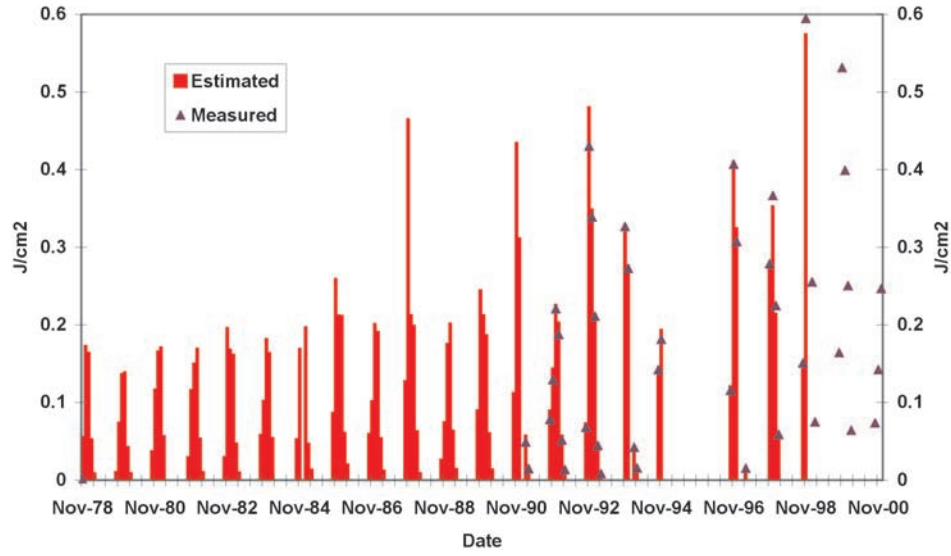

Figure 7. Daily integrated irradiance 303.030–307.692 nm, monthly mean, estimated from CMDL/NOAA pyranometer and measured by spectroradiometer SUV-100/NSF, when available.

Day for the estimated values in the period 1978–1998 are shown, which do not show considerable dispersion. Also, historical maximum and minimum values for each Julian Day for the measured spectral irradiances (SUV-100) in the period 1991–2000 are shown in the same figure. It may be observed that extreme historical daily values for both time series do not differ significantly, which suggests that the results observed in the model test can be extrapolated. From the geophysical point of view, this figure is also relevant, since it suggests that for the period 1978–1998, no trend is observed in the cloud attenuation effect at South Pole.

[38] Finally, the regression equation was applied to estimate daily integrated irradiances in the (303.030–307.692 nm) band from November 1978 to December 1998. Figure 6 shows this modelled time series, and the measured SUV-100 values, where available, for South Pole. A significant increment is observed since 1985, reaching a more stable situation in the middle nineties, which is consistent with ozone depletion events. Monthly mean time series of irradiances are shown in Figure 7, where the increase, in this case, is evident since 1987. Some abnormal situations are observed in Barrow since 1990, but the increase is not as evident and does not appear each year as at South Pole.

[39] Considering that the most critical events that affect the ozone column occur in October at South Pole and April at Barrow, monthly means for these months were plotted in Figure 8. At South Pole, an upward trend is observed in the October means since 1983, with an increasing variability after 1987, in accordance with ozone values. As a consequence, October monthly means since the late 1980s are around 300% larger than during the late 1970s and early 1980s at that site. At Barrow, on the other hand, larger values are observed for 1990 and 1993, between 90 and 120% larger than values in the early 1980s, which are related to ozone depletion. This statement is based in the fact that ozone monthly means are lower those years and

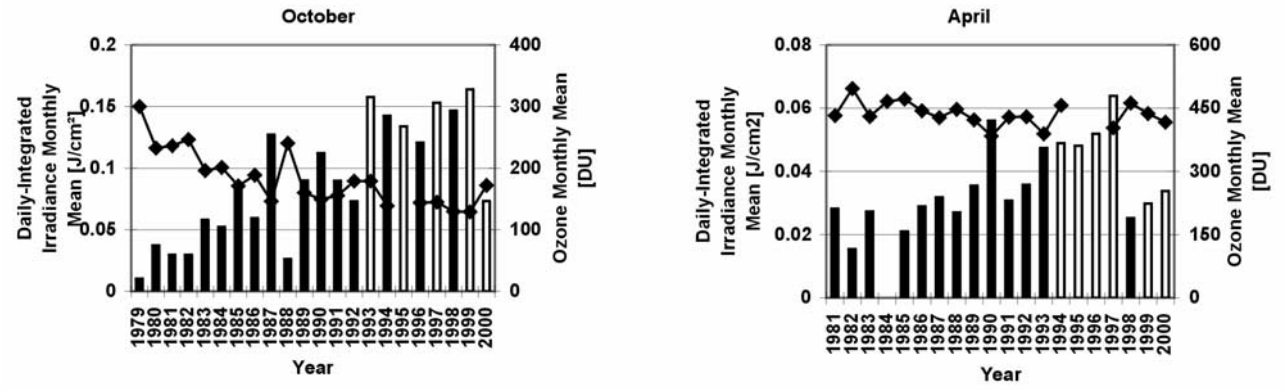

Figure 8. Daily integrated irradiance 303.030–307.692 nm, monthly mean, estimated from CMDL/NOAA pyranometer (solid bars) and, completing time series with values measured by spectroradiometer SUV-100/NSF (open bars). Secondary axis shows monthly average of daily ozone total column from satellite (TOMS) (diamonds). (left) October at South Pole. (right) April at Barrow.

monthly global irradiances (from CDML pyranometers) do not show significant changes relative to other years. In this paper, only a brief analysis of South Pole and Barrow time series is shown, and a more detailed study is being prepared, which will be presented in a future publication.

4. Conclusions

[40] A multiregressive model was presented to estimate spectral, narrowband or biologically weighted irradiances as a function of total column ozone, broadband irradiances and solar zenith angles.

[41] The model was solved and tested using various combinations of narrowband and broadband irradiances, total column ozone, weather, ground albedo and solar zenith angles. Results suggest that the model may be reliable for any site, since no restrictions were applied to sky conditions, ground albedos or solar zenith angles. Differences due to possible slight variations between instruments in the collector response or calibration standards did not result in important changes in the RMS relative errors.

[42] This model can be applied to improve existing broadband instrument networks by adding, for example, a travelling multichannel or spectral instrument. Since the same methodology can be applied for different type of broadband instruments, it would even be possible to convert different type of well-calibrated independent instruments into a network, adding a travelling instrument, as pointed out above. Also, the existence of long-term well calibrated broadband instruments time series can be considered as a factor of decision, when the sites to install new spectral or multichannel instruments have to be chosen.

[43] Finally, the model was used to estimate historical narrowband data back to 1978 for South Pole and Barrow. Model results suggest that the monthly mean daily integrated irradiance at South Pole for the (303.030–307.692 nm) band during October, would be around 300% higher since late eighties relative to the late 1970s, while increases between 90 and 120% are present at Barrow during some spring periods.

[44] **Acknowledgments.** This publication was partially supported by the CRN–026 of the Inter-American Institute for Global Change. The authors want to thank P. Penhale and NSF Polar Programs, and CADIC/CONICET for their support to perform this study. They also want to thank C. R. Booth and the UV Group, Biospherical Instruments Inc (BSI), San Diego for providing the irradiance databases and R. Mc Peters and J. Herman, NASA GSFC for providing total column ozone. In addition, the authors are grateful to NOAA/CMDL for providing the broadband irradiance data for South Pole.

References

Bodecker, G. E., and R. L. Mc Kenzie, An algorithm for inferring surface UV irradiance including cloud effects, *J. Appl. Meteorol.*, *35*, 1860–1877, 1996.

Booth, C. R., T. B. Lucas, J. H. Morrow, C. S. Weiler, and P. A. Penhale, The United States National Science Foundation 's Polar Network for monitoring ultraviolet radiation, in *Ultraviolet Radiation in Antarctica: Measurements and Biological Effects*, *Antarctic Res. Ser.*, vol. 62, edited by C. S. Weiler and P. A. Penhale, pp. 17–37, AGU, Washington, D. C., 1994.

Booth, C. R., J. E. Ehramjian, T. Mestechkina, L. W. Cabasug, J. S. Robertson, and J. R. Tusson, NSF Polar programs UV spectroradiometer network 1995–1997 operations report, report, 241 pp., Biospher. Instrum. Inc., San Diego, Calif., 1998.

Callis, L. B., M. Natarajan, and J. D. Lambeth, Calculated upper stratospheric effects of solar UV flux and NO_Y variations during the 11-year solar cycle, *Geophys. Res. Lett.*, *27*, 3869–3872, 2000.

Cebula, R. P., E. Hilsenrath, and M. T. Deland, Middle ultraviolet solar spectral irradiance measurements, 1985-1992, from SBUV/2 and SSBUV instruments, in *The Sun as Variable Star: Solar and Stellar Variations*, edited by J. M. Pap et al., pp. 81–88, Cambridge Univ. Press, New York, 1994.

Cebula, R. P., G. O. Thuillier, M. E. Van Hoosier, E. Hilsenrath, M. Herse, G. E. Brueckner, and P. C. Simon, Observation of the solar irradiance in the 200–350 nm interval during the Altas-1 mission: A comparison among three sets of measurements: SSBUV, SOLPEC, and SUSIM, *Geophys. Res. Lett.*, *23*, 2289–2292, 1996.

Chandra, S., and R. D. McPeters, The solar cycle variation of ozone in the stratosphere inferred from Nimbus 7 and NOAA 11 satellites, *J. Geophys. Res.*, *99*, 20,665–20,671, 1994.

Chubarova, N. Y., N. A. Krotkov, I. V. Geogdzhaev, T. K. Kondranin, and V. U. Khattatov, Spectral UV Irradiance: The effects of ozone, cloudiness and surface albedo, in *Proceedings IRS'96: Current Problems in Atmospheric Radiation*, pp. 881–885, A. Deepak, Hampton, Va., 1997.

Cutchis, A., Formula for comparing actual damaging ultraviolet (DUV) radiation doses at tropical and mid-latitude sites, *Fed. Aviation Admin. Rep.FAA-EE 80-21*, U. S. Dep. of Transport., Washington D. C., 1980.

den Outer, P. N., H. Slaper, J. Matthijsen, H. A. J. M. Reinen, and R. Tax, Variability of ground- level ultraviolet: Model and measurement, *Radiat. Prot. Dosimetry*, *91*(1–3), 105–110, 2000.

Diaz, S. B., C. R. Booth, T. B. Lucas, and I. Smolskaia, Effects of ozone depletion on irradiances and biological doses over Ushuaia, *Adv. Limnol.*, *43*, 115–122, 1994.

Diaz, S. B., G. Deferrari, D. Martinioni, and A. Oberto, Regresión análisis of biologically effective integrated irradiances versus ozone, clouds and geometric factors, *J. Atmos. Sol. Terr. Phys.*, *62*, 629–638, 2000.

Eck, T. F., P. K. Bhartia, and J. B. Kerr, Satellite estimation of spectral UVB irradiance using TOMS derived total ozone and UV reflectivity, *Geophys. Res. Lett.*, *22*, 611–614, 1995.

Erlick, C., and J. E. Frederick, Effects of aerosols on the wavelength dependence of atmospheric transmission in the ultraviolet and visible, 2, Continental and urban aerosols in clear skies, *J. Geophys. Res.*, *103*, 23,275–23,285, 1998.

Estupinan, J. G., S. Raman, G. H. Crescenti, J. J. Streitcher, and W. F. Barnard, The effects of clouds and haze on UV-B radiation, *J. Geophys. Res.*, *101*, 807–816, 1996.

Fioletov, V. E., J. B. Kerr, and D. I. Wardle, The relationship between total ozone and spectral UV irradiance from Brewer observations and its use for derivation of total ozone from UV measurements, *Geophys. Res. Lett.*, *24*, 2997–3000, 1997.

Fioletov, V. E., L. J. B. McArthur, J. B. Kerr, and D. I. Wardle, Estimation of long-term changes in ultraviolet radiation over Canada, paper presented at Quadriennial Ozone Symposium, Int. Ozone Comm., Sapporo, Japan, 2000.

Frederick, J. E., and C. Erlick, The Attenuation of sunlight by high-latitude clouds: Spectral dependence and its physical mechanisms, *J. Atmos. Sci.*, *54*, 2813–2819, 1997.

Frederick, J. E., and H. D. Steele, The transmission of sunlight through cloudy skies: An analysis based on standard meteorological information, *J. Appl. Meteorol.*, *34*, 2755–2761, 1995.

Frölich, C., Variability of the solar constant on time scales of minutes to years, *J. Geophys. Res.*, *92*, 796–800, 1987.

Herman, J. R., P. K. Barthia, O. Torres, C. Hsu, C. Seftor, and E. Celarier, Global distribution of UV-absorbing aerosols from Nimbus 7 TOMS data, *J. Geophys. Res.*, *102*, 16,911–16,922, 1997.

Huang, T. Y. W., The impact of solar radiation on the quasi-biennial oscillation of the ozone in the tropical stratosphere, *Geophys. Res. Lett.*, *23*, 3211–3214, 1996.

Ilyas, M., Effect of cloudiness on solar ultraviolet radiation reaching the surface, *Atmos.*, *21*, 1483–1484, 1987.

Ilyas, M., A. Pandy, and M. S. Jaafar, Changes to the surface level solar ultraviolet-B radiation due to haze perturbation, *J. Atmos. Chem.*, *40*, 111–121, 2001.

Ito, T., Y. Sakoda, T. Uekubo, H. Naganuma, M. Fukuda, and M. Hayashi, Scientific application of UV-B observations from JMA network, paper presented at 13th UOEH International Symposium and the 2nd Pan Pacific Cooperative Symposium on Human Health and Ecosystems, UOEH, Kitakyushu, Japan, 1994.

Josefsson, W. A. P., Solar ultraviolet radiation in Sweden, *SMHI Rep. 53*, Natl. Inst. of Radiat. Prot. in Stockholm, Norrköping, Sweden, 1986.

Krorkov, N. A., P. K. Barthia, J. B. Herman, V. Fioletov, and J. Kerr, Satellite estimation of spectral surface UV irradiance in the presence of tropospheric aerosols, 1, Cloud-free case, *J. Geophys. Res.*, *103*, 8779–8793, 1998.

Kylling, A., A. Albod, and G. Seckmeyer, Transmittance of a cloud is wavelength-dependent in the UV- range: Physical interpretation, *Geophys. Res. Lett.*, *24*, 397–400, 1997.

Kylling, A., A. F. Bais, M. Blumthaler, J. Schreder, C. S. Zerefos, and E. Kosmidis, Effect of aerosols on solar UV irradiances during the Photochemical Activity and Solar Ultraviolet Radiation campaign, *J. Geophys. Res.*, *103*, 26,051–26,060, 1998.

Lean, L. J., G. J. Rottman, H. L. Kyle, T. N. Woods, J. R. Hickey, and L. C. Puga, Detection and parameterization of variations in solar mid- and near-ultraviolet radiation (200–400 nm), *J. Geophys. Res.*, *102*, 29,939–29,956, 1997.

Li, Z., P. Wang, and J. Cihlar, A simple and efficient method for retrieving surface UV radiation dose rate from satellite, *J. Geophys. Res.*, *105*, 5027–5036, 2000.

McArthur, L. J. B., V. E. Fioletov, J. B. Kerr, C. T. Mc Elroy, and D. J. Wardle, Derivation of UV-A irradiance from pyranometer measurements, *J. Geophys. Res.*, *104*, 30,139–30,151, 1999.

McPeters, R., P. K. Barthia, A. J. Krueger, J. R. Herman, Nimbus-7 Total Ozone Mapping Spectrometer (TOMS): Data product user's guide, *NASA Ref. Publ.*, *1384*, 1996.

McPeters, R., P. K. Barthia, A. J. Krueger, and J. R. Herman, Earth Probe Total Ozone Mapping Spectrometer (TOMS): Data product user's guide, *NASA Tech. Publ.*, 1998-206895, 1998.

Mo, T., and A. E. S. Green, A climatology of solar erythema dose, *Photochem. Photobiol.*, *20*, 483–496, 1974.

Nelson, D. W., The NOAA Climate Monitoring and Diagnostic Laboratory Solar Radiation Facility, *NOAA Tech. Memo. OAR CMDL15*, 2000.

Randell, W. J., and F. Wu, Isolation of the ozone QBO in SAGE II data by singular-value decomposition, *J. Atmos. Sci.*, *53*, 2546–2559, 1996.

Seckmeyer, G., R. Erb, and A. Albod, Transmittance of a cloud is wavelength-dependent in the UV-range, *Geophys, Res. Lett.*, *23*, 2753–2755, 1996.

Wardle, D. L., J. B. Kerr, C. T. McElroy, and D. R. Francis, Ozone science: Canadian perspective on the changing ozone layer, 119 pp., Environ. Canada, Toronto, Ontario, Canada, 1997.

Warren, S. G., C. J. Hahn, J. London, R. M. Chervin, and R. L. Jenne, Global distribution of total cloud cover and cloud type amounts over land, *NCAR Tech. Rep. NCAR/TN-273 + STR*, Natl. Cent. of Atmos. Res., Boulder, Colo., 1986.

Zerefos, C., C. Meleti, D. Balis, K. Tourpali, and A. F. Bais, Quasibiennial and longer-term changes in clear sky UV-B solar irradiance, *Geophys. Res. Lett.*, *25*, 4345–4348, 1998.

Zhou, S., G. J. Rottman, and A. J. Miller, Stratospheric ozone response to short- and intermediate-term variations of solar UV flux, *J. Geophys. Res.*, *102*, 9003–9011, 1997.

Zhou, S., A. J. Miller, and L. L. Hood, A partial correlation analysis of the stratospheric ozone response to 12-day solar UV variations with temperature effect removed, *J. Geophys. Res.*, *105*, 4491–4500, 2000.

C. Camillón, Centro Austral de Investigaciones Científicas/IAI, Ruta 3 y Cap. Mutto, (9410) Ushuaia, Tierra del Fuego, Argentina. (carolinacamilion@hotmail.com)

G. Deferrari, Centro Austral de Investigaciones Científicas/NSF, Ruta 3 y Cap. Mutto, (9410) Ushuaia, Tierra del Fuego, Argentina. (defe@infovia.com.ar)

S. Díaz, Centro Austral de Investigaciones Científicas/CONICET, Ruta 3 y Cap. Mutto, (9410) Ushuaia, Tierra del Fuego, Argentina. (subediaz@stalink.com)

D. Nelson, National Oceanic and Atmospheric Administration/CMDL, 325 Broadway, R/CMDL, Boulder, CO 80305, USA. (dnelson@cmdl.noaa.gov)